ELSEVIER

Agriculture, Ecosystems and Environment 94 (2003) 205–220

Agriculture Ecosystems & Environment

www.elsevier.com/locate/agee

Remote sensing of regional crop production in the Yaqui Valley, Mexico: estimates and uncertainties

David B. Lobell [a,*], Gregory P. Asner [a,1], J. Ivan Ortiz-Monasterio [b], Tracy L. Benning [c]

[a] *Department of Geological Sciences and Environmental Studies Program, Campus Box 399, Benson Earth Sciences Building, University of Colorado, Boulder, CO 80309-0399, USA*

[b] *International Maize and Wheat Improvement Center (CIMMYT), Wheat Program, Apdo. Postal 6-641, 06600 Mexico D.F., Mexico*

[c] *Department of Environmental Science, Policy, and Management, University of California, Berkeley, CA 94720, USA*

Received 15 June 2001; received in revised form 6 December 2001; accepted 20 February 2002

Abstract

Quantifying crop production at regional scales is critical for a wide range of applications, including management and carbon cycle modeling. Remote sensing offers great potential for monitoring regional production, yet the uncertainties associated with large-scale yield estimates are rarely addressed. In this study, we estimated crop area, yield, and planting dates for 2 years of Landsat imagery in an intensive agricultural region in northwest Mexico. Knowledge of crop phenology was combined with multi-temporal imagery to estimate crop rotations throughout the region. Remotely sensed estimates of the fraction of absorbed photosynthetically active radiation (fAPAR) were then incorporated into a simple model based on crop light-use efficiency to predict yield and planting dates for wheat. Uncertainty analysis revealed that regional yield predictions varied up to 20% with the method used to determine fAPAR from satellite, but were relatively insensitive to modeled variability in crop phenology, light-use efficiency, and harvest index (the ratio of grain mass to aboveground biomass). Comparisons of satellite-based and field-based estimates indicated errors in regional wheat yields of less than 4% for both years of data. In contrast, planting date calculations exhibited uncertainties of up to 50% using a sparse, three-date sampling from satellite-based sensors. A simplified model was also developed to explore yield predictions using only one date of imagery, demonstrating high accuracies depending on the date of image acquisition. The spatial and temporal distributions of crop production derived here offer valuable information for agricultural management and biogeochemical modeling efforts, provided that their uncertainties are well understood.
© 2002 Elsevier Science B.V. All rights reserved.

Keywords: Crop yield; NPP; Remote sensing; Wheat; Radiation use efficiency; Uncertainty analysis

1. Introduction

Regional estimates of crop yield are desirable for managing large agricultural lands and determining food pricing and trading policies (Macdonald and Hall, 1980; Hutchinson, 1991). In addition, knowledge of crop extent and productivity can provide critical inputs to meteorological and biogeochemical models. For example, modeled contamination

* Corresponding author. Present address: Department of Global Ecology, Carnegie Institution of Washington, Stanford, CA 94305, USA.

E-mail address: dlobell@globalecology.stanford.edu (D.B. Lobell).

[1] Present address: Department of Global Ecology, Carnegie Institution of Washington, Stanford, CA 94305, USA.

0167-8809/02/$ – see front matter © 2002 Elsevier Science B.V. All rights reserved.
PII: S0167-8809(02)00021-X

of water with nitrate is strongly dependent on the spatial distributions of crops within an agricultural region (Beaujouan et al., 2001). The regional carbon (C) balance of agriculture is of particular interest to global biogeochemical research and greenhouse gas emission policy, as increased production and reduced tillage have led to significant accumulations of C in several field studies (Lal et al., 1995; Buyanovsky and Wagner, 1998). Quantifying the impacts of management practices on regional C balance is critical for establishing emission policies, yet a reliable methodology for assessing regional C dynamics remains to be realized (Subak, 2000; Post et al., 2001).

C storage in agriculture is defined as the difference between C fluxes into and out of the soil, since annual harvesting prevents any long-term storage in aboveground biomass. Inputs are provided by crop residues remaining after harvest, while outputs consist of soil heterotrophic respiration (R_h) and leaching of dissolved organic carbon (DOC) (Fig. 1). Numerous models have been developed to simulate R_h and DOC leaching processes and their responses to management (e.g., Parton et al., 1994; Neff and Asner, 2001). However, most models rely on relatively simple treatments of input fluxes (but see Asner et al. (2001)), which can exhibit high spatial and temporal variability in agroecosystems (Plant et al., 1999).

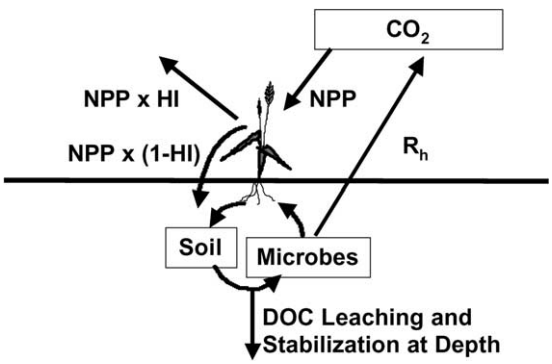

Fig. 1. A simple representation of the C cycle in agriculture. Soil C storage is the balance between input and output fluxes, with input fluxes controlled by the amount of total NPP and the fraction removed as harvest (HI). Output fluxes include heterotrophic respiration by microbes (R_h) and DOC leaching and stabilization at depth, neglecting fluxes due to erosion. Knowledge of spatial and temporal variations in NPP is needed for both accurate yield estimates and quantifying C balance.

An important step towards quantifying regional C balance is therefore an accurate assessment of net CO_2 uptake in crop growth, termed net primary production (NPP). This task consists of (1) identifying the spatial extent of different crops and (2) estimating production per unit area of each crop. Regional crop area and NPP estimates based on field reports are often expensive, prone to large errors, and cannot provide the real-time, spatially explicit estimates or predictions of yield needed to establish food policies or monitor C fluxes (Reynolds et al., 2000). Satellite remote sensing is an attractive tool for crop area and NPP estimates because it provides spatial and temporal information on the location and state of crop canopies (Kumar and Monteith, 1981; Moulin et al., 1998). However, successful use of remote sensing requires that remotely measured radiance can be accurately related to physical plant properties and that these properties can then be related to NPP or yield. Hereafter, production is discussed mainly in terms of yield for comparison with field data, although NPP is directly related to yield according to the fraction of plant biomass that is harvested (harvest index, HI) and the carbon fraction of biomass by weight (∼45%, Schlesinger, 1997).

The dynamics of regional yields and agricultural NPP are exemplified in the Yaqui Valley, an intensive wheat-based agricultural region in Sonora, Mexico. The Yaqui Valley consists of approximately 226,000 ha between the Rio Yaqui and Rio Mayo, and is adjacent to the Gulf of California (27°N, 110°W; Fig. 2). The home of the Green Revolution, it is agro-climatically representative of ∼34 million ha of irrigated spring wheat, where over 40% of the developing world's wheat is produced (Pingali and Rajaram, 1999). Farmers in Yaqui Valley typically apply 250 kg nitrogen (N) ha^{-1} and irrigate wheat crops 4–5 times during the growing season, resulting in some of the highest wheat yields in the world (FAO, 1997), as well as extremely high nitrogen trace gas (N_2O, NO) fluxes (Matson et al., 1998). Secondary crops include safflower, spring cotton, fall maize and summer soybean, although changing water policies and reduced water availability have caused farmers to abandon summer cropping since 1998. Management changes from field to field and year to year emphasize the need for a regional perspective to estimate yields and NPP.

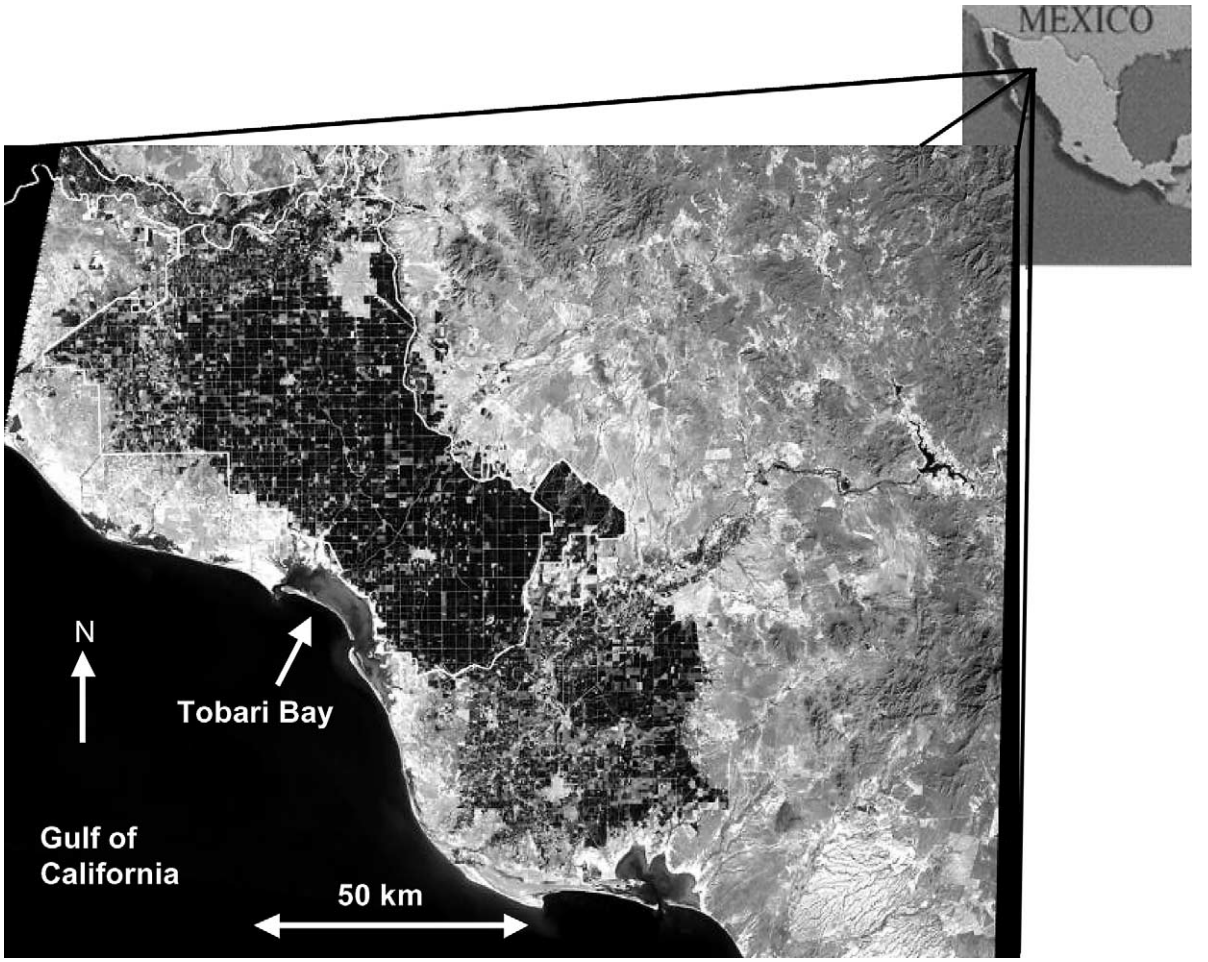

Fig. 2. Yaqui Valley study region, as seen from Landsat ETM+ band 3 image on February 26, 2000. Wheat fields are dark due to the strong absorption by vegetation at visible wavelengths. A GIS coverage outlining the Yaqui agricultural district is overlaid in white.

1.1. Remote sensing of yield

A simple and useful paradigm for modeling crop yield with remote sensing is derived from Monteith (1972, 1977):

$$\text{Yield} = \text{APAR} \times \varepsilon \times \text{HI} \quad (1)$$

where APAR is the total amount of photosynthetically active radiation (PAR) (MJ from 400 to 700 nm) absorbed by a canopy throughout the growing season, ε the light-use efficiency in units of g biomass MJ^{-1} PAR, and HI the harvest index or ratio of grain mass to aboveground biomass. In this case, as in most studies, HI and ε refers only to aboveground biomass and does not include roots.

Numerous studies have demonstrated that ε is a relatively constant property of plants, since light harvesting is often adjusted to the availability of resources needed to use the absorbed light (Monteith, 1977; Russell et al., 1989; Bloom et al., 1985; Field et al., 1995). Thus, variations in plant production should be reflected mainly by changes in APAR, which can be monitored from remote sensing platforms (Kumar and Monteith, 1981). However, uncertainty in each of the variables in Eq. (1) must be addressed to determine if this approach can be used for accurate yield estimates,

or if a more mechanistic treatment of plant light-use is needed (Moulin et al., 1998). For example, variability in ε and HI can result from a variety of nutrient, water, and temperature stresses (Russell et al., 1989; Hay, 1995; Sinclair and Muchow, 1999), but the degree to which these factors affect yield estimates in highly managed systems is unknown.

Measurements of APAR represent another source of error for yield estimates, and are usually estimated as the product of incident PAR and the fraction of photosynthetically active radiation (fAPAR) absorbed by the canopy, summed over the growing season:

$$\text{APAR} = \sum(\text{PAR} \times \text{fAPAR})\Delta t \quad (2)$$

Several field studies have used daily measurements of PAR and fAPAR to assess crop production (Gallagher and Biscoe, 1978; Garcia et al., 1988; Gallo et al., 1993), but satellite observations are generally not available at daily frequencies. Global sensors, such as the advanced very high resolution radiometer (AVHRR), offer fAPAR estimates at daily to biweekly intervals, but the low spatial resolutions (>1 km) of these sensors cannot capture relevant spatial patterns within agricultural regions. Higher resolution satellites, such as Landsat Thematic Mapper (TM) with 30 m resolution, are usually only available a few times per year for a given location. This is due to the lower revisit time of Landsat-class sensors (~16 days) and the frequency of cloud cover. To utilize the high spatial resolution of Landat-type sensors, estimates from select dates throughout the growing season can be used with a predefined time-profile of fAPAR based on field studies to estimate daily fAPAR, which can then be used in Eq. (2) (e.g., Leblon et al., 1991). Since high spatial resolution is essential for studying regional patterns in NPP, this is the approach adopted in this study.

However, differences between field and remote sensing measurements of fAPAR introduce another source of uncertainty when combining the two to estimate yield. In the field, fAPAR is most often substituted with the fraction of intercepted photosynthetically active radiation (fIPAR), calculated from PAR measurements above and below the canopy:

$$\text{fIPAR} = \frac{\text{PAR}_{\text{above}} - \text{PAR}_{\text{below}}}{\text{PAR}_{\text{above}}} \quad (3)$$

The functional fAPAR in Eq. (2), i.e., PAR absorbed by photosynthetic tissues, is usually within 10% of fIPAR (Russell et al., 1989) but can differ significantly due to canopy and soil reflectance (Prince, 1991) and absorption by non-photosynthetic tissues (Asner et al., 1998), with the latter becoming very significant during senescence (e.g., Asrar et al., 1984). Remote sensing estimates of fAPAR (e.g., Asrar et al., 1984; Steinmetz et al., 1990; Wiegand et al., 1992) have their own uncertainties due to imperfect relationships between combinations of red and near-infrared (NIR) reflectance, called spectral vegetation indices (SVI), and fAPAR. Some commonly employed SVI include the simple ratio (SR) and normalized difference vegetation index (NDVI):

$$\text{SR} = \frac{\text{NIR}}{\text{red}} \quad (4)$$

$$\text{NDVI} = \frac{\text{NIR} - \text{red}}{\text{NIR} + \text{red}} \quad (5)$$

Several authors suggest on theoretical and empirical grounds that SR is best related to fAPAR (e.g., Steinmetz et al., 1990; Serrano et al., 2000), while others have supported the use of NDVI (Asrar et al., 1984; Gallo et al., 1993). Still others indicate that an average of SR and NDVI performs the best (Los et al., 2000), leaving great ambiguity as to the appropriate measure of fAPAR.

The goal of this study was to quantify the accuracy and precision of regional crop rotation, yield and planting date estimates from remote sensing. Yield and planting date estimates focused on wheat, with only area estimated for other crops, since wheat is by far the dominant crop in Yaqui Valley (in terms of food supply, farmer income and NPP; Naylor et al., 2001). Uncertainties in ε, HI and both field and remotely sensed estimates of fAPAR for wheat were defined and propagated with a Monte Carlo technique to quantify the resulting confidence in estimates, and thereby assess the true utility of Eq. (1) for regional yield predictions. Model results were then compared to field-based planting and harvest reports. In addition, yield estimates using a single image and several simplifying assumptions were considered to assess the impact of limited data availability.

2. Methods

2.1. Field measurements

To determine the time-profile of APAR for wheat, field measurements of incident solar radiation and canopy interception were recorded during the 1994–1995 growing season for bread wheat grown on research plots at the International Maize and Wheat Improvement Center (CIMMYT) in Yaqui Valley. All plots were planted on November 28, 1994 and were irrigated five times according to common farmer practices. Four separate plots grown at varying levels of fertilization (0, 85, 167 and 250 kg N ha^{-1}) were assessed to determine the effect of nutrient levels on fAPAR, ε and HI. Daily solar radiation was measured by a pyranometer (LI-200SA, Li-COR, Lincoln, Nebraska), with downwelling PAR values computed by multiplying solar shortwave radiation by 0.48 (Szeicz, 1974). fIPAR was measured within 1 h of local noon on January 4, 12, 19, February 1, 11, 14, 22, 28, and March 7 and 23, 1995, using a canopy analyzer (Sunfleck Ceptometer, Decagon, Pullman, WA) above and below the canopies. The daily fIPAR time-profile was estimated using linear interpolation between measurements, with time defined by growing degree days (GDD) rather than calendar days to account for changes in crop development due to accumulated temperature (Ritchie and NeSmith, 1991).

Field fIPAR was converted to fAPAR by assuming that 5% of intercepted light is reflected or absorbed by non-photosynthetic tissues when the canopy is completely green (Asner et al., 1998), and that this percentage increases during senescence (Asrar et al., 1984; see Fig. 2B). To determine fAPAR during senescence, a simple linear interpolation from 5% at the onset of senescence to 100% at physiological maturity, when wheat is fully senesced, was used to define the fraction of fIPAR that is not absorbed by photosynthetic elements. The onset of senescence was observed between 1 and 2 weeks before maturity in field studies, although uncertainty in the date of onset was also considered (see below).

In addition to radiation measurements, final biomass and grain yield were evaluated to determine values of ε and HI. Plots were hand harvested after physiological maturity, with total wet biomass for the harvested area (4.5 m^2) measured in the field and a sub-sample of 100 stems taken to determine moisture content. After several days of sun drying, threshing took place and grain weight was recorded. ε was determined as the ratio of biomass to APAR, while HI was equal to grain mass (0% moisture) divided by total dry biomass.

2.2. Satellite measurements of croplands

Two separate years of satellite data were tested in this study. Landsat 5 TM images were acquired for 1993–1994 on October 12, 1993, and February 1, April 6, and July 27, 1994; Landsat 7 Enhanced Thematic Mapper Plus (ETM+) images were acquired on October 12 and December 24, 1999, and February 26 and April 16, 2000 for the 1999–2000 season. To determine the location and areal extent of each major crop, the images were first coregistered to within one pixel error using ground control points, and then georeferenced by matching geographic information system (GIS) road and drainage canal coverages to image features. All pixels within the Yaqui Valley agricultural district were defined using an additional GIS layer of district boundaries (see Fig. 2).

The SR was used to distinguish pixels with actively growing crops from bare soil in each image, using a simple threshold value (see Fig. 4 below). Crop rotations were then determined by classifying the time-profile of crop presence (Table 1). For example, pixels with high SR in the October and July images from 1993 to 1994 were interpreted as fall maize–summer soybean rotations, while pixels with high SR in February and July were considered winter wheat–summer soybean rotations. This approach ignored the presence of senescent canopies and crops not included in Table 1, but provided a simple means to estimate crop area with the available images.

2.3. Yield and planting date estimates

To determine yield, fAPAR was calculated in each image as a linear function of SR, following Sellers et al. (1996):

$$\mathrm{fAPAR} = \frac{(\mathrm{SR} - \mathrm{SR}_{\min})(\mathrm{fAPAR}_{\max} - \mathrm{fAPAR}_{\min})}{(\mathrm{SR}_{\max} - \mathrm{SR}_{\min})} + \mathrm{fAPAR}_{\min} \quad (6)$$

where SR is the value of the simple ratio at a given pixel, $\mathrm{SR}_{\min}$ and $\mathrm{SR}_{\max}$ correspond to the second and

Table 1
Growing season of major crops in Yaqui Valley, and greenness (Y/N) during image acquisition dates used to determine crop areas

Crop	Growing season	October 12	December 24	February 1	February 26	April 6	April 16	July 27
Maize	August–January	Y/N[a]	Y	N	N	N	N	N
Wheat	November–May	N	Y/N[a]	Y	Y	Y/N[b]	Y/N[b]	N
Soybean	May–September	N	N	N	N	N	N	Y

[a] Some fields may remain in early stages of development and thus may not appear green.
[b] Some fields may already be senescent at this date and thus may not appear green.

98th percentile of SR for the entire agricultural region, and $fAPAR_{min}$ and $fAPAR_{max}$ are defined as 0.01 and 0.95, respectively. SR_{min} and SR_{max} were computed separately for each image to avoid errors due to structural differences between crops and different stages of development. As discussed, several studies suggest that replacing SR with NDVI in Eq. (5) results in more accurate fAPAR estimates (Choudhury, 1987; Goward and Huemmrich, 1992). We therefore calculated fAPAR both ways and compared the resulting yield estimates. We also used fAPAR computed as the average fAPAR from SR and NDVI, following Los et al. (2000). The three methods are hereafter referred to as fAPAR−SR, fAPAR−NDVI, and fAPAR−(SR−NDVI), respectively.

The satellite estimates of fAPAR at each pixel were then used to adjust the field-based time-profile of wheat fAPAR, and thereby estimate daily fAPAR throughout the growing season. In this case, since at least two images were available for both the years (February 1 and April 6 for 1993–1994; December 24, February 26 and April 16 for 1999–2000), we varied two properties of the fAPAR profile; the initial day of growth or planting date (d), which is important for determining the light and temperature regime for plant development, and the maximum canopy fAPAR (f_{max}). f_{max} and d were determined for each pixel as the combination which minimized the sum of squared differences between the fAPAR profile and satellite estimates. APAR was then calculated from Eq. (2) using the computed profile of fAPAR with station measured daily PAR, and yield was determined from Eq. (1).

As mentioned, a primary goal of this study was to quantify potential uncertainties in yield and planting date estimates from Landsat data. We first considered uncertainties in fixed model inputs (i.e., inputs that did not change from image to image), including the length of senescence and the method used to estimate satellite fAPAR. For simplicity, three dates of senescence onset (1, 2 and 3 weeks before maturity) and three fAPAR models (fAPAR−SR, fAPAR−NDVI and fAPAR−(SR−NDVI)) were tested, with a total of nine possible combinations for each year. For each combination, we then quantified uncertainties arising at the image scale, namely potential bias in fAPAR estimates, and at the pixel scale, including variance in fAPAR and $\varepsilon \times$ HI. Bias in fAPAR was considered because errors in $fAPAR_{min}$, $fAPAR_{max}$, SVI_{min} and SVI_{max} in Eq. (6) can lead to systematic over- or underestimates of fAPAR within an image. Variance in fAPAR, or scatter in the linear relationship in Eq. (6), arises from many sources including variable background reflectance, atmospheric effects and canopy structural differences (Myneni and Williams, 1994). Variance in $\varepsilon \times$ HI is due to the factors discussed in Section 1, and was defined here as observed variability within the different N treatments. The quantity $\varepsilon \times$ HI was used rather than treating ε and HI separately to accommodate any dependence between them in field data.

The impacts of the above listed uncertainties on yield and planting date estimates were quantified using a Monte Carlo technique. Model predictions were repeated many times, each time with random perturbations to fAPAR, ε and HI generated from distributions representing their variability. Normally distributed random variables with standard deviations (σ) of 0.05 and 0.10 were used to generate fAPAR bias and scatter, respectively, while σ for $\varepsilon \times$ HI was derived from field results (see below). A large number of model runs was performed ($n = 100$) for each pixel to ensure that the computed mean and σ for yield and planting date converged. Values of σ for fAPAR bias and scatter were conservatively largely based on previous studies (e.g., Asrar et al., 1984; Steinmetz et al.,

1989; Wiegand et al., 1992; Los et al., 2000), so that the resulting uncertainty in yield and planting date estimates were also considered conservative.

2.4. Single image yield estimates

The utility and optimal timing of a single image for yield estimates are important to consider for future applications, since factors such as expense and cloud cover often inhibit satellite data availability. In this context, a simple model was also tested in which the planting date was assumed constant for all fields, and the estimated fAPAR from the February image was used to calculate f_{max} in Eq. (6) and thus yield. The sensitivity of yield estimates to planting date was considered by calculating yield for each planting date from November 15 to January 15. In addition, the sensitivity to image date was assessed by comparing results for the 2 years, where 1994 and 2000 had an early and late February acquisition date, respectively.

3. Results and discussion

3.1. Field measurements

Differences between N treatments were reflected in field measurements of fIPAR, as predicted by the resource balance perspective (Fig. 3A). The differences were the greatest between the control ($0\,kg\,N\,ha^{-1}$) and $85\,kg\,N\,ha^{-1}$ treatments, and noticeably smaller between the higher N treatments. Biomass differences were similarly greater between the lower N treatments (Table 2), indicating a decreasing marginal return at high levels of N application. ε values computed from integrated growing season APAR and final biomass measurements ($2.2–2.4\,g\,MJ^{-1}$ PAR) were similar to previous studies of wheat, which generally report light-use efficiencies in the range of $2–3\,g\,MJ^{-1}$ PAR (Gallagher and Biscoe, 1978; Garcia et al., 1988; Kiniry et al., 1989).

Analysis of field data revealed no apparent dependence of ε or HI on N treatment (Table 2). This finding is consistent with several studies that show N has a small and often insignificant effect on light-use efficiency (Garcia et al., 1988; Steinmetz et al., 1990; Serrano et al., 2000). Variability of ε and HI within different treatments was generally low (~2 and 3% of their respective means), and variability of their product was also low (3% of the mean), indicating that higher harvest indices partially compensated for low light-use efficiencies. This result may reflect a physiological mechanism for decreased HI with increased production (Hay, 1995), or may simply express the codependence of ε and HI on biomass measurements, with underestimates in biomass leading to low ε but high HI. Regardless, $\varepsilon \times$ HI was described by a

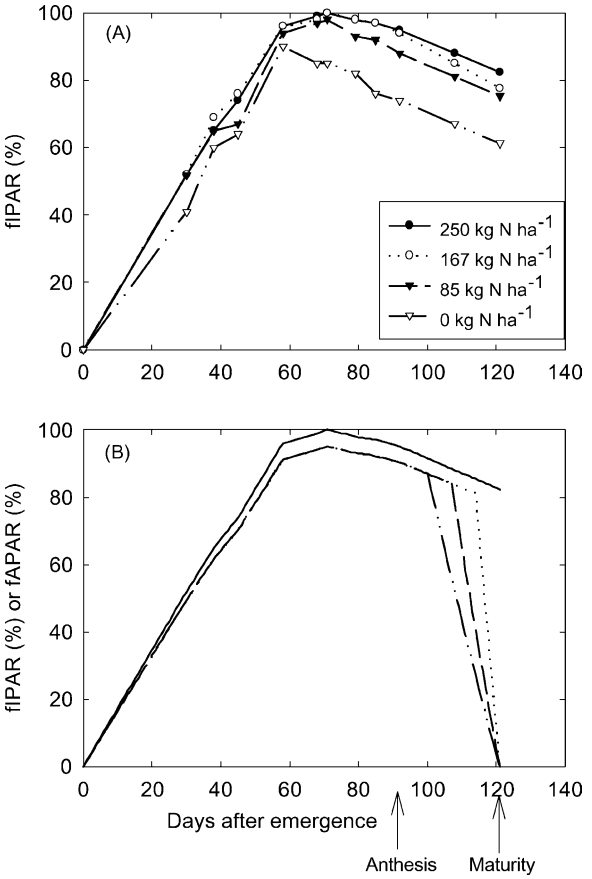

Fig. 3. (A) Measured fIPAR for four different nitrogen (N) treatments throughout 1994–1995 growing season. Dates of anthesis (flowering) and maturity observed in the field are shown. fIPAR at maturity was not directly measured, but interpolated linearly from the previous two measurements. fIPAR at emergence was assumed to be zero. (B) A comparison of measured fIPAR (solid line) and estimated fAPAR for the $250\,kg\,N\,ha^{-1}$ treatment, assuming 1 (dotted), 2 (dashed) and 3 weeks (dashed-dot) of senescence. fAPAR prior to senescence was assumed 95% of fIPAR, resulting in a maximum fAPAR of 0.95.

Table 2
Field estimates and variability of HI and light-use efficiency (ε) for four nitrogen (N) treatments (values were calculated assuming 1, 2 and 3 weeks of senescence)

N treatment	Biomass ($g\,m^{-2}$)	Yield	HI[a]	$APAR_1$[b,c]	ε_1[d]	$\varepsilon_1 \times HI$	$APAR_2$	ε_2	$\varepsilon_2 \times HI$	$APAR_3$	ε_3	$\varepsilon_3 \times HI$
0	1239.4	488.7	0.394	569	2.178	0.859	543	2.283	0.900	517	2.397	0.945
85	1489.1	543.8	0.365	658	2.263	0.826	626	2.379	0.869	595	2.503	0.914
167	1480.5	551.1	0.372	689	2.149	0.800	654	2.264	0.843	622	2.380	0.886
250	1509.9	560.7	0.371	694	2.176	0.808	659	2.291	0.851	625	2.416	0.898
Mean	1429.7	536.1	0.376	652.5	2.191	0.824	620.5	2.304	0.866	589.8	2.424	0.911
Standard deviation.	127.5	32.4	0.012	57.9	0.050	0.026	53.7	0.051	0.026	50.3	0.054	0.026

[a] Harvest index: ratio of grain mass to aboveground biomass (unitless).
[b] Absorbed photosynthetically active radiation for entire growing season (MJ PAR).
[c] Subscript indicates assumed date of onset of senescence in weeks before maturity.
[d] Light-use efficiency ($g\,MJ^{-1}$ PAR).

normal distribution with $\sigma = 3\%$ of the mean (with the mean determined by the weeks of senescence) for the Monte Carlo analysis.

3.2. Crop rotations

Fields with actively growing crops were clearly distinguished from bare soils using a threshold of SR = 2, due to the bimodal distribution of SR within the agricultural region (Fig. 4). The estimated area of harvested crops from this approach was within 5% of the reported areas for wheat, and within 3% for soybean (Table 3). Larger errors were observed for maize (∼50%), due to the fact that image acquisition (October 12 for both the years) was much earlier than the peak of the maize growth cycle, so that many maize fields did not appear green in the image (see Table 1). While these errors would be improved with more frequent observations, the low errors for wheat and soybean were deemed highly useful since these were the two dominant crops in the region.

The spatial distribution of crop rotations inferred for 1993–1994 is shown in Fig. 5. The dominant rotation throughout the valley was wheat–soybean, with approximately 78,000 ha attributed to this rotation. The spatially explicit information in Fig. 5 was not available from field data, preventing any direct comparison but highlighting the unique capabilities of remote sensing. Crop rotations in Fig. 5 provide valuable information for land-use assessments and modeling efforts. For example, different crop types can be associated with different tillage, fertilizer and irrigation practices, providing spatial constraints on management practices that are needed in biogeochemical models (e.g., Parton et al., 1994).

3.3. Yield and planting date estimates

The results of the Monte Carlo analysis revealed several interesting properties of the yield estimates (Table 4). First, yield assessments were primarily sensitive to the method used to compute fAPAR, with a difference of ∼20% between those based on SR and NDVI. The most accurate estimates resulted from fAPAR−(SR−NDVI), supporting the combined use of SR and NDVI for fAPAR measurements (Los et al., 2000). Assumptions about the onset of senescence had a smaller effect on yield, with changes of only ∼5% between estimates using 1 and 3 weeks of senescence. In addition, yield predictions were rather insensitive to image and pixel level perturbations to fAPAR and changes in $\varepsilon \times HI$, with σ only ∼5% of the mean.

Mean yield estimates using fAPAR−(SR−NDVI) agreed well with reported values, differing by only 3.3% for 1993–1994 and −0.3% for 1999–2000, assuming 1 week of senescence. Moreover, the distributions of yield within Yaqui Valley were consistent with field observations, which generally exhibited minimum and maximum yields around 4.0 and 7.5 $t\,ha^{-1}$, respectively (Fig. 6). The distributions also revealed interesting differences between the two growing seasons that could not be obtained from total harvest data.

Fig. 7 shows the frequency histograms for yield and month of planting date for the Monte Carlo

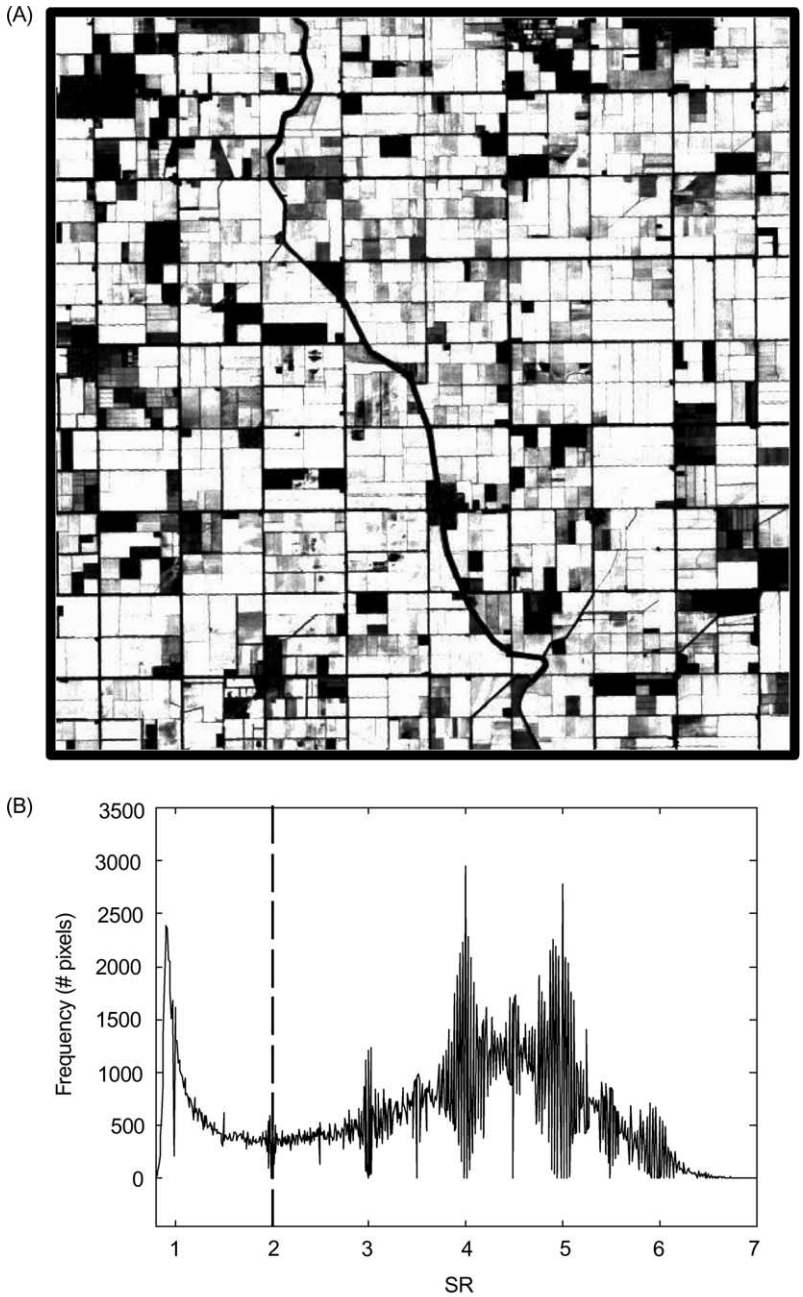

Fig. 4. (A) February 26, 2000 SR image for a representative subset of Yaqui Valley, showing the distinction between cropped and bare fields. The image is scaled from SR = 0 (black) to 4 (white), with gray fields comprised of wheat in early stages of development. (B) Histogram of image in (A), demonstrating bimodal distribution of SR. Dashed line at SR = 2 shows threshold used to identify active crops.

Table 3
Comparison of crop areas estimated from Landsat data with harvested areas reported by the Yaqui Valley agricultural district

Crop	Growing Season	Reported area (ha)	Estimated area (ha)	Difference (%)
Maize	1993–1994	58377	34117	42
Wheat	1993–1994	152751	157939	3
Soybean	1993–1994	120127	124091	3
Maize	1999–2000	4414	1516	66
Wheat	1999–2000	191281	182247	5

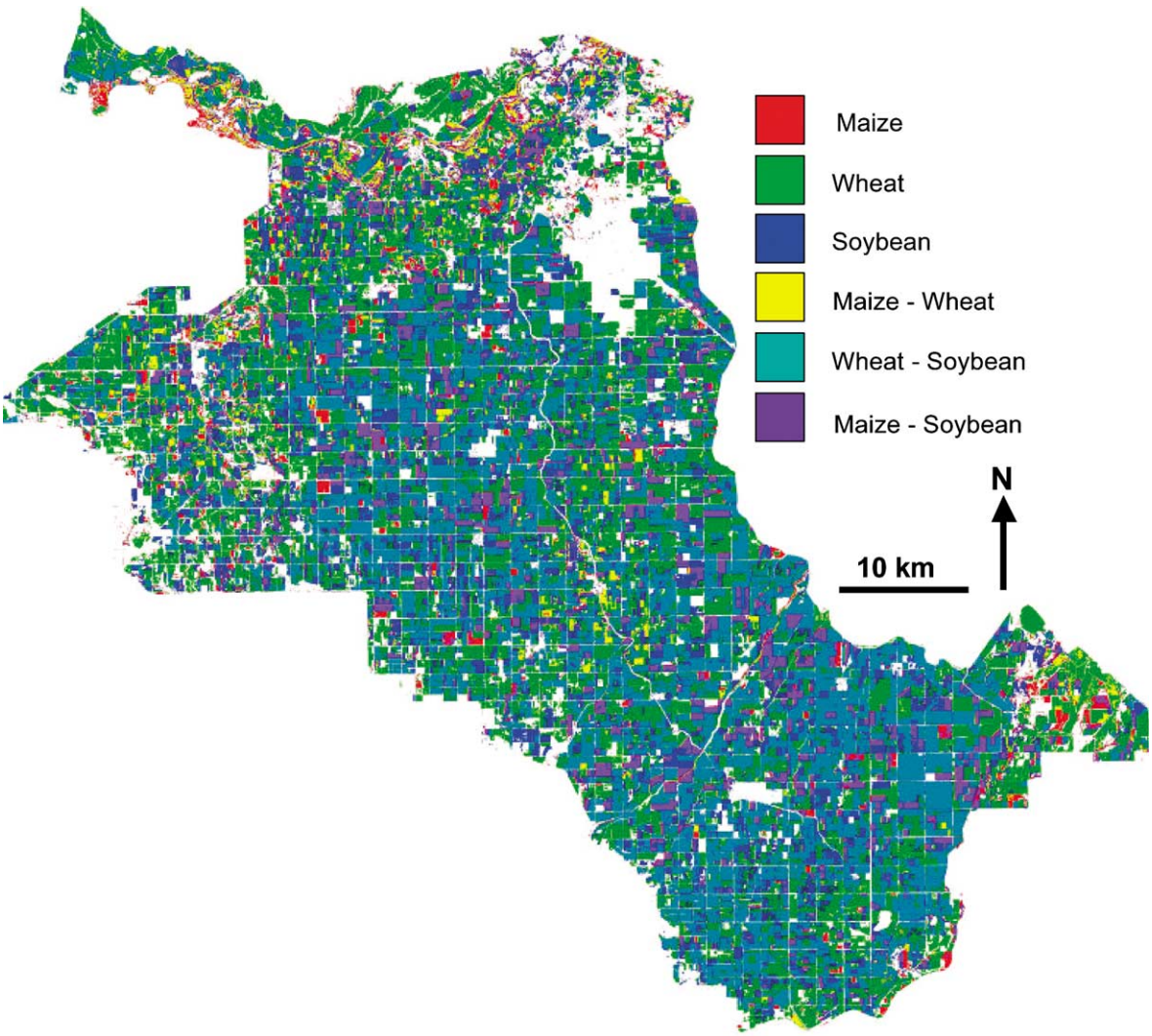

Fig. 5. Crop rotations for 1993–1994 in Yaqui Valley agricultural district inferred from multi-temporal Landsat data and crop phenologies. White areas, such as the large canal through the center of the valley and the urban area (Ciudad Obregon) in the northeast, indicate where no crops were detected.

Table 4
Means and standard deviations (parentheses) of yield estimates (metric tons) from Monte Carlo analysis, for three fAPAR methods and three dates of senescence[a]

Growing season	Weeks senesced	Reported	fAPAR−SR	fAPAR−NDVI	fAPAR−(SR−NDVI)[b]
1993–1994	1	823399	758965 (26117)[c]	943298 (28658)	850217 (30772)
	2	823399	798049 (32182)	987438 (25860)	882930 (33711)
	3	823399	828624 (34564)	1019619 (23868)	911537 (38616)
1999–2000	1	1082542	977704 (44511)	1195076 (47437)	1079190 (41316)
	2	1082542	994700 (39268)	1242416 (37955)	1107893 (49720)
	3	1082542	1010330 (44026)	1267287 (40437)	1124336 (47520)

[a] Reported values from agricultural district data are shown for comparison. All yield estimates were divided by 0.88 for comparison with reported grain yields, which are at 12% moisture.
[b] Average fAPAR from SR and NDVI.
[c] Value in parenthesis is 1 standard deviation.

analysis using the fAPAR−(SR−NDVI) relationship and assuming 1 week of senescence. Reported yield and planting months, shown by the dark vertical lines, were all within the range estimated by the Monte Carlo analysis. However, while the uncertainty in yield estimates were fairly low ($\sigma \sim 5\%$ of mean), planting months could not be predicted with high confidence (σ up to 50% of mean; see Table 5). Moreover, both the assumed length of senescence and the fAPAR method had relatively strong effects on predicted planting months (Table 5).

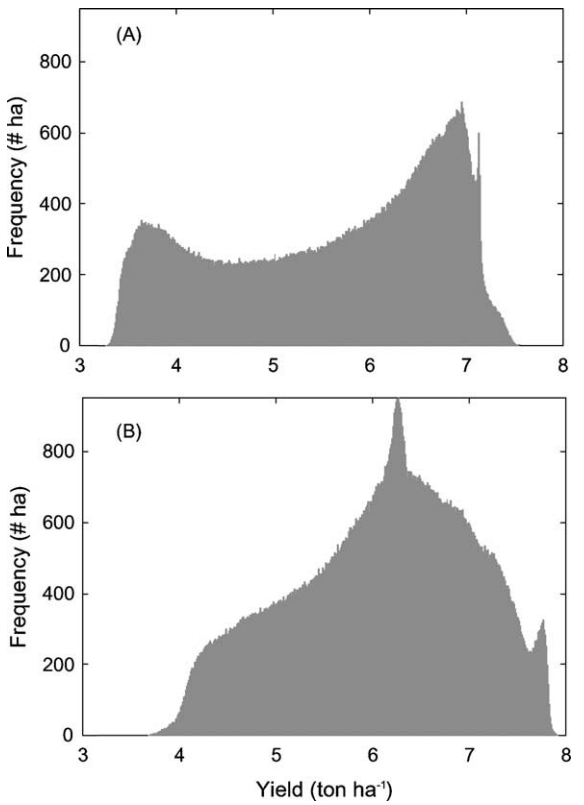

Fig. 6. Histograms of (A) 1993–1994 and (B) 1999–2000 mean wheat yield estimates for Yaqui Valley, assuming 1 week of senescence and using fAPAR−(SR−NDVI).

The low confidence in planting date estimates would almost certainly be improved with more observations during the initial stages of development (Moulin et al., 1998; Guérif and Duke, 2000). While high frequency observations are generally not available from Landsat and other high spatial resolution sensors, global sensors such as the AVHRR offer more frequent observations at low spatial resolutions (>1 km). Using information from Landsat about the spatial extent of crops within AVHRR pixels, it is therefore feasible to improve estimates of crop phenology with course resolution sensors (e.g., Fisher, 1994). However, the results here emphasize that modeled uncertainty in crop phenology does not have a large effect on yield estimates. Therefore, a relevant question is not only how well can we estimate planting dates but also how poorly can we assume planting dates and still have confidence in yields?

3.4. Single image yield estimates

Yield estimates from the simple model with fixed planting dates are shown in Fig. 8. Of particular interest here is the potential accuracy of yield predictions assuming that all fields were planted on a single

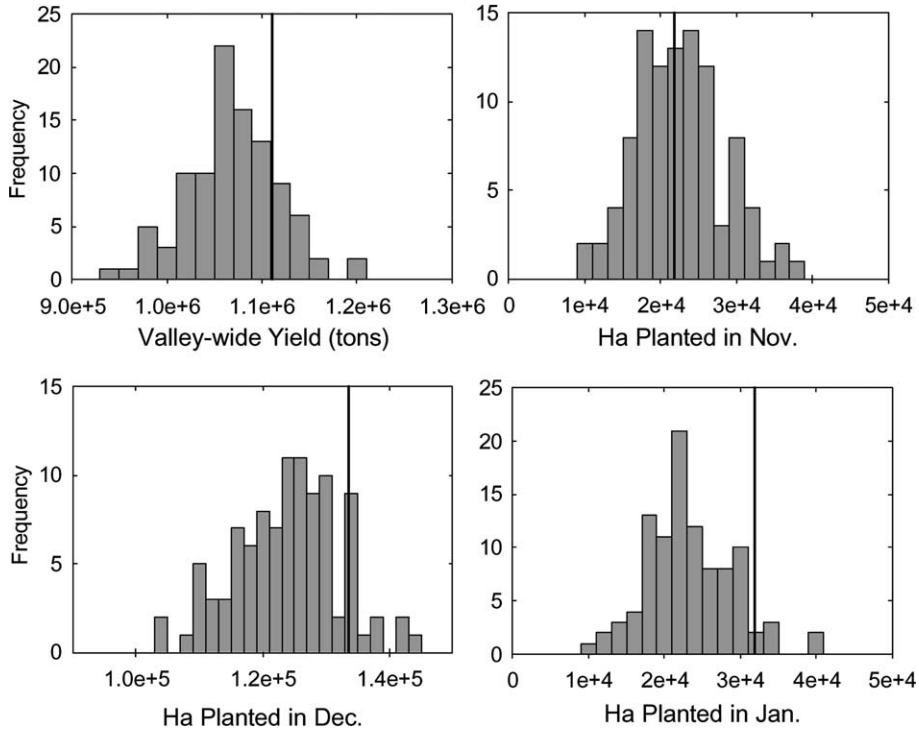

Fig. 7. Histograms of 1999–2000 yield and planting months calculated in Monte Carlo analysis ($n = 100$), assuming 1 week of senescence and using fAPAR−(SR−NDVI). Solid vertical lines indicate reported values from district data.

date. Again, assessments using SR and NDVI under- and overestimated actual yields, respectively, in both the years of data by ∼10%, while an average fAPAR from SR and NDVI resulted in more accurate yields. In 1999–2000, estimates were not very sensitive to the assumed planting date over a reasonable range of dates (e.g., December 1–January 1). For example, the average planting date appears to be around December 10, but assuming a date of December 20 would result in only ∼3% error.

In contrast, yield estimates for 1993–1994 were much more sensitive to planting date, with a 10-day

Table 5
Means and standard deviations of 1999–2000 planting date month estimates from Monte Carlo analysis[a]

fAPAR method/weeks senesced	Hectares planted in November	Hectares planted in December	Hectares planted in January
Reported	21572	133270	31609
SR/1	24240 (5652)[b]	114430 (8069)	33461 (6603)
SR/2	27496 (7704)	109382 (10478)	35541 (6487)
SR/3	35958 (9835)	107318 (11688)	34478 (7462)
NDVI/1	22186 (5096)	135264 (6718)	15992 (4376)
NDVI/2	31222 (6581)	132690 (6870)	16182 (4398)
NDVI/3	34863 (5665)	130684 (7862)	16434 (4706)
SR−NDVI/1	23073 (5741)	126117 (8139)	23795 (4503)
SR−NDVI/2	29589 (6292)	122737 (7892)	24889 (5169)
SR−NDVI/3	34940 (6744)	117734 (8093)	26108 (5467)

[a] Reported values from agricultural district data are shown for comparison.
[b] Value in parenthesis is 1 standard deviation.

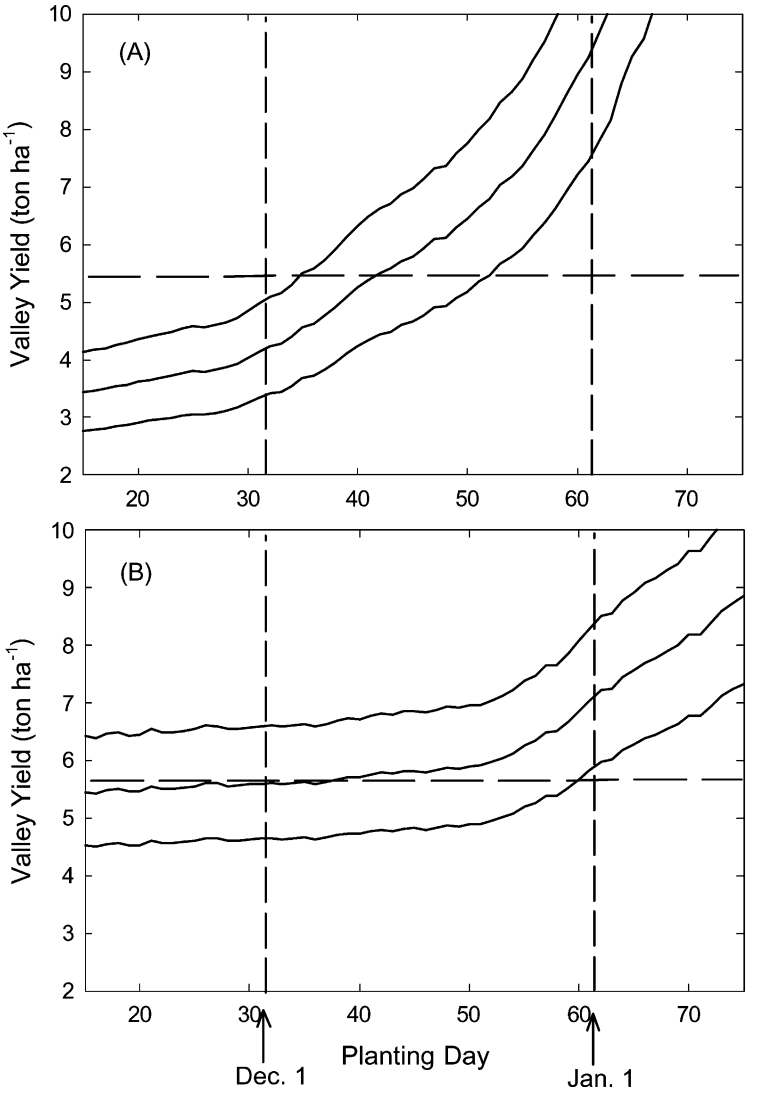

Fig. 8. (A) 1993–1994 yield estimates (average t ha^{-1}) for a range of assumed planting dates, using an image acquired on February 1, 1994. Lower, middle and upper lines correspond to estimates using fAPAR−SR, fAPAR−(SR−NDVI) and fAPAR−NDVI, respectively. Horizontal dashed line indicates reported mean yield from district data. (B) Same as in (A) but for 1999–2000, using an image acquired on February 26, 2000.

error in assumed planting date resulting in ∼27% error in yield. The differences between the 2 years are explained by the dates on which in the images were acquired. February 1 is still before the peak in fAPAR for most planting dates (e.g., February 1 is 58 days after emergence in Fig. 3), while most wheat canopies are fully developed by February 26. Therefore, wheat planted 10 days apart will look more similar on February 26 than February 1, causing errors in the assumed planting date to have less impact for the later image. These results suggest that yield can be accurately estimated with a single image and a reasonable assumption for planting date, provided that the image is acquired towards the middle of the growing season when most canopies are fully developed.

3.5. Other potential sources of error

While this study considered several potential sources of error, namely variability in ε and HI and errors in fAPAR measurements, several others remained unmodeled due to a lack of sufficient field data. For example, bias in the estimates of ε and HI could result from interannual changes in practices, cultivars or environmental conditions (e.g., Choudhury, 2000). In fact, field records indicate the harvest indices were slightly lower in 1999–2000 than in 1994–1995 (Ortiz-Monasterio, unpublished data), which interestingly explains the slight overestimates of yield for the 1999–2000 data (Table 3). In addition, changes in the timing of canopy development, for instance due to a shift from bread wheat to durum wheat, could impact yield and planting month estimates. However, the accurate yield estimates calculated here suggest that any unmodeled sources of error were relatively minor and should not hinder future predictions of yield in this area.

The utility of the approach presented here in other agricultural regions will depend on additional uncertainties. Most notably, widespread irrigation in the Yaqui Valley prevented significant water stress, which can have a substantial effect on ε (Steinmetz et al., 1990; Sinclair and Muchow, 1999) and would require explicit consideration through soil moisture models or thermal remote sensing (Guérif et al., 1993). The absence of serious crop diseases, weeds or pest infestations was also a simplifying factor in Yaqui Valley, and such factors may need to be considered to the extent that their effects are not captured in variations in fAPAR. Another important issue for any approach based on satellite reflectance measurements is persistent cloud cover during the growing season, such as those occurring throughout much of the tropics. While cloud cover was not a problem in this study, the modeling framework developed here is capable of incorporating images from any point in the growing season and provides an estimate of uncertainty that depends, among other things, on the timing of images relative to the crop growth cycle. Overall, the generality and relative simplicity of this modeling approach should facilitate applications to other crops and regions, where additional sources of uncertainty should be carefully considered and quantified in order to determine the full potential of remotely sensed yield estimates.

4. Conclusions

The accuracy and low uncertainty of yield estimates in this study strongly support the use of Eq. (1) for regional yield studies. In addition, our results indicate that accurate yield predictions are possible using only one image, provided that it is acquired near the peak of development for most fields. The incorporation of fAPAR from scaled vegetation indices in this study offers a distinct advantage over yield models that require estimates of leaf area index, since the latter approach relies on often difficult and inaccurate atmospheric corrections (e.g., Bouman, 1992; Clevers and van Leeuwen, 1996; Bach, 1998).

The spatial distributions of crop rotations and production can be used for a variety of applications. Future work will focus on incorporating NPP estimates with a biogeochemical model to predict regional C storage, and on using remotely sensed patterns of yield to investigate sources of variability within and between fields. However, one must be careful to consider potential uncertainties in derived parameters, as demonstrated by the low precision of planting date estimates. Applications in new regions may need to consider additional sources of uncertainty such as water stress (Guérif et al., 1993), which was not a factor in this well irrigated region.

Acknowledgements

We thank P. Matson for helpful comments on the manuscript, and A. Townsend and J. White for logistical support. This work was supported by a NSF Graduate Research Fellowship, a NSF-IGERT grant to the University of Colorado, and NASA New Investigator Program grant NAG5-8709.

References

Asner, G.P., Wessman, C.A., Archer, S., 1998. Scale dependence of absorption of photosynthetically active radiation in terrestrial ecosystems. Ecol. Appl. 8 (4), 1003–1021.

Asner, G.P., Townsend, A.R., Riley, W.J., Matson, P.A., Neff, J.C., Cleveland, C.C., 2001. Physical and biochemical controls over terrestrial ecosystem responses to nitrogen deposition. Biogeochemistry 54 (1), 1–39.

Asrar, G., Fuchs, M., Kanemasu, E.T., Hatfield, J.L., 1984. Estimating absorbed photosynthetically active radiation and leaf

area index from spectral reflectance in wheat. Agron. J. 76, 300–306.

Bach, H., 1998. Yield estimation of corn based on multitemporal Landsat-TM data as input for an agrometeorological model. Pure Appl. Opt. 7, 809–825.

Beaujouan, V., Durand, P., Ruiz, L., 2001. Modelling the effect of the spatial distribution of agricultural practices on nitrogen fluxes in rural catchments. Ecol. Model. 137, 93–105.

Bloom, A.J., Chapin, F.S., Mooney, H.A., 1985. Resource limitation in plants: an economic analogy. Annu. Rev. Ecol. Syst. 16, 363–392.

Bouman, B.A.M., 1992. Linking physical remote sensing models with crop growth simulation models, applied for sugar beet. Int. J. Remote Sens. 13, 2565–2581.

Buyanovsky, G.A., Wagner, G.H., 1998. Changing role of cultivated land in the global carbon cycle. Biol. Fert. Soils 27, 242–245.

Choudhury, B.J., 1987. Relationships between vegetation indices, radiation absorption, and net photosynthesis evaluated by a sensitivity analysis. Remote Sens. Environ. 22, 209–233.

Choudhury, B.J., 2000. A sensitivity analysis of the radiation use efficiency for gross photosynthesis and net carbon accumulation by wheat. Agric. For. Meteorol. 101, 217–234.

Clevers, J.G.P.W., van Leeuwen, H.J.C., 1996. Combined use of optical and microwave remote sensing data for crop growth monitoring. Remote Sens. Environ. 56, 42–51.

Field, C.B., Randerson, J.T., Malmström, C.M., 1995. Global net primary production: combining ecology and remote sensing. Remote Sens. Environ. 51 (1), 74–88.

Fisher, A., 1994. A simple model for the temporal variations of NDVI at regional scale over agricultural countries-validation with ground radiometric measurements. Int. J. Remote Sens. 15, 1421–1446.

Food and Agriculture Organization, 1997. FAOSTAT. Rome.

Gallagher, J.N., Biscoe, P.V., 1978. Radiation absorption, growth and yield of cereals. J. Agric. Sci. 91, 47–60.

Gallo, K.P., Daughtry, C.S.T., Wiegand, C.L., 1993. Errors in measuring absorbed radiation and computing crop radiation use efficiency. Agron. J. 85, 1222–1228.

Garcia, R., Kanemasu, E.T., Blad, B.L., Bauer, A., Hatfield, J.L., Major, D.J., Reginato, R.J., Hubbard, K.G., 1988. Interception and use efficiency of light in winter wheat under different nitrogen regimes. Agric. For. Meteorol. 44, 175–186.

Goward, S.N., Huemmrich, K.F., 1992. Vegetation canopy PAR absorptance and the normalized difference vegetation index: an assessment using the SAIL model. Remote Sens. Environ. 39, 119–140.

Guérif, M., Duke, C.L., 2000. Adjustment procedures of a crop model to the site specific characteristics of soil and crop using remote sensing data assimilation. Agric. Ecosyst. Environ. 81, 57–69.

Guérif, M., Brisis, S.D., Seguin, B., 1993. Combined NOAA-AVHRR and SPOT-HRV data for assessing crop yields of semiarid environments. EARSeL Adv. Remote Sens. 2, 110–123.

Hay, R.K.M., 1995. Harvest index: a review of its use in plant breeding and crop physiology. Ann. Appl. Biol. 126, 197–210.

Hutchinson, C.F., 1991. Uses of satellite data for famine early warning in sub-Saharan Africa. Int. J. Remote Sens. 12, 1405–1421.

Kiniry, J.R., et al., 1989. Radiation-use efficiency in biomass accumulation prior to grain-filling for five grain species. Field Crops Res. 20, 51–64.

Kumar, M., Monteith, J.L., 1981. Remote sensing of crop growth. In: Smith, H. (Ed.), Plants and the Daylight Spectrum. Academic Press, London, pp. 133–144.

Lal, R., Kimble, J.M., Levine, E.R., Stewart, B.A., 1995. Soil Management and Greenhouse Effect. CRC Press, Boca Raton, FL, 385 pp.

Leblon, B., Guérif, M., Baret, F., 1991. The use of remotely sensed data in estimation of PAR use efficiency and biomass production of flooded rice. Remote Sens. Environ. 38, 147–158.

Los, S.O., et al., 2000. A global 9-year biophysical land surface dataset from NOAA AVHRR data. J. Hydrometeorol. 1, 183–199.

Macdonald, R.B., Hall, F.G., 1980. Global crop forecasting. Science 208 (4445), 670–679.

Matson, P.A., Naylor, R., Ortiz-Monasterio, J.I., 1998. Integration of environmental, agronomic, and economic aspects of fertilizer management. Science 280, 112–114.

Monteith, J.L., 1972. Solar radiation and productivity in tropical ecosystems. J. Appl. Ecol. 9, 747–766.

Monteith, J.L., 1977. Climate and the efficiency of crop production in Britain. Phil. Trans. Roy. Soc. Lond. B 281, 277–294.

Moulin, S., Bondeau, A., Delecolle, R., 1998. Combining agricultural crop models and satellite observations: from field to regional scales. Int. J. Remote Sens. 19 (6), 1021–1036.

Myneni, R.B., Williams, D.L., 1994. On the relationship between FAPAR and NDVI. Remote Sens. Environ. 49, 200–211.

Naylor, R.L., Falcon, W.P., Puente-Gonzalez, A., 2001. Policy reforms and Mexican agriculture: views from the Yaqui Valley. Economics Program Paper No. 01-01. CIMMYT, Mexico D.F.

Neff, J.C., Asner, G.P., 2001. Dissolved organic carbon in terrestrial ecosystems: synthesis and a model. Ecosystems 4, 29–48.

Parton, W.J., Ojima, D.S., Cole, C.V., Schimel, D.S., 1994. A general model for soil organic matter dynamics: sensitivity to litter chemistry, texture, and management. In: SSSA (Ed.), Quantitative Modeling of Soil Forming Processes. Soil Science Society of America, Madison, pp. 147–167.

Pingali, P.L., Rajaram, S., 1999. Global wheat research in a changing world: options and sustaining growth in wheat productivity. In: Pingali, P.L. (Ed.), CIMMYT 1998–1999 World Wheat Facts and Trends. CIMMYT, Mexico D.F.

Plant, R.E., Mermer, A., Pettyfrove, G.S., Vayssieres, M.P., Young, J.A., Miller, R.O., Jackson, L.F., Denison, R.F., Phelps, K., 1999. Factors underlying grain yield spatial variability in three irrigated wheat fields. Trans. ASAE 42 (5), 1187–1202.

Post, W.M., Izaurralde, R.C., Mann, L.K., Bliss, N., 2001. Monitoring and verifying changes of organic carbon in soil. Climatic Change 51 (1), 73–99.

Prince, S.D., 1991. A model of regional primary production for use with coarse-resolution satellite data. Int. J. Remote Sens. 12, 1313–1330.

Reynolds, C.A., Yitayew, M., Slack, D.C., Hutchinson, C.F., Huete, A., Petersen, M.S., 2000. Estimating crop yields and production by integrating the FAO crop specific water balance model with real-time satellite data and ground-based ancillary data. Int. J. Remote Sens. 21 (18), 3487–3508.

Ritchie, J.T., NeSmith, D.S., 1991. Temperature and crop development. In: Hanks, J., Ritchie, J.T. (Eds.), Modeling Plant and Soil Systems. Agronomy Monograph No. 31. ASA, CSSA, SSSA, Madison, WI.

Russell, G., Jarvis, P.G., Monteith, J.L., 1989. Absorption of radiation by canopies and stand growth. In: Russell, G., Marshall, B., Jarvis, P.G. (Eds.), Plant Canopies: Their Growth, Form and Function. Cambridge University Press, Cambridge, pp. 21–39.

Schlesinger, W.H., 1997. Biogeochemistry: An Analysis of Global Change. Academic Press, San Diego, 443 pp.

Sellers, P.J., et al., 1996. A revised land surface parameterization (SiB2) for atmospheric GCMs. Part 1. Model formulation. J. Climate 9, 676–705.

Serrano, L., Fillela, I., Penuelas, J., 2000. Remote sensing of biomass and yield of winter wheat under different nitrogen supplies. Crop Sci. 40, 723–731.

Sinclair, T.R., Muchow, R.C., 1999. Radiation use efficiency. Adv. Agron. 65, 215–265.

Steinmetz, S., Guerif, M., Delecolle, R., Baret, F., 1990. Spectral estimates of the absorbed photosynthetically active radiation and light-use efficiency of a winter wheat crop subjected to nitrogen and water deficiencies. Int. J. Remote Sens. 11, 1797–1808.

Subak, S., 2000. Agricultural soil carbon accumulation in North America: considerations for climate policy. Global Environ. Change 10, 185–195.

Szeicz, G., 1974. Solar radiation for plant growth. J. Appl. Ecol. 11, 617–637.

Wiegand, C.L., Maas, S.J., Aase, J.K., Hatfield, J.L., Pinter Jr., P.J., Jackson, R.D., Kanemasu, E.T., Lapitan, R.L., 1992. Multisite analyses of spectral-biophysical data for wheat. Remote Sens. Environ. 42, 1–21.